Isoginkgetin, a bioactive constituent from *Ginkgo Biloba,* protects against obesity-induced cardiomyopathy via enhancing Nrf2/ARE signaling

Xiaoqian Wu [a,b,1,*], Jianrong Huang [a,1], Junyuan Tang [a], Yuling Sun [a], Guojun Zhao [b], Cuishi Yan [a], Zhenghong Liu [c], Wei Yi [a], Suowen Xu [c,**], Xiyong Yu [a,***]

[a] *Key Laboratory of Molecular Target & Clinical Pharmacology and the State & NMPA Key Laboratory of Respiratory Disease, School of Pharmaceutical Sciences& the Fifth Affiliated Hospital, Guangzhou Medical University, Guangzhou, 511436, China*
[b] *The Sixth Affiliated Hospital of Guangzhou Medical University, Qingyuan People's Hospital, Qingyuan, 511500, China*
[c] *Department of Endocrinology, The First Affiliated Hospital of USTC, Division of Life Sciences and Medicine, University of Science and Technology of China (USTC), Hefei, 230037, China*

A B S T R A C T

Obesity-induced metabolic cardiomyopathy (MC), characterized by lipotoxicity and excessive oxidative stress, emerges as the leading cause of heart failure in the obese patients. Yet, its therapy remains very limited. Here, we demonstrated that isoginkgetin (IGK), a bioactive biflavonoid isolated from medicinal herb *Ginkgo Biloba,* protected against obesity-induced cardiac diastolic dysfunction and adverse remodeling. Transcriptomics profiling revealed that IGK activated Nrf2 signaling in the heart tissues of the obese mice. Consistent with this observation, IGK treatment increased the nuclear translocation of Nrf2, which in turn trigger the activation of its downstream target genes (e. g. HO-1 and NQO1). In addition, IGK significantly rejuvenated mitochondrial defects in obese heart tissues as evidenced by enhancing mitochondrial respiratory capacity and resisting the collapse of mitochondrial potential and oxidative stress both *in vitro* and *in vivo*. Mechanistically, IGK stabilized Nrf2 protein via inhibiting the proteasomal degradation, independent of transcription regulation. Moreover, molecular docking and dynamics simulation assessment demonstrated a good binding mode between IGK and Nrf2/Keap1. Of note, the protective effects conferred by IGK against obesity-induced mitochondrial defects and cardiac dysfunction was compromised by Nrf2 gene silencing both *in vitro* and *in vivo*, consolidating a pivotal role of Nrf2 in IGK-elicited myocardial protection against MC. Thus, the present study identifies IGK as a promising drug candidate to alleviate obesity-induced oxidative stress and cardiomyocyte damage through Nrf2 activation, highlighting the therapeutic potential of IGK in ameliorating obesity-induced cardiomyopathy.

1. Introduction

Obesity is still an ongoing epidemic worldwide. To date, more than one third of US adults are obese. A cross-sectional survey of the general US population from the National Health and Nutrition Examination Survey demonstrated that obesity escalates among adolescents and adults in the US from 1999 to 2018 [1]. Growing evidence has suggested that patients of obesity are more susceptible to develop metabolic cardiomyopathy (MC), which occurred in the absence of coronary artery disease, valvular heart disease, hypertension, and other cardiovascular disease [2–4]. Multiple obesity-related deleterious factors, including insulin resistance, altered substrate utilization, overt oxidative stress and mitochondrial dysfunction, are pivotal contributors to cardiac dysfunction, and eventually heart failure (HF) [3,5]. Over half of the HF patients are either obese or diabetic and HF is emerging as the leading cause of mortality in these patients [6,7]. The prevalence of MC is expected to escalate in parallel with obesity; however, precise cures for obesity MC remain elusive, and therapeutic tools are of urgent medical need in this setting.

Despite the fact that the molecular basis of obesity-driven MC is

---

poorly understood, accumulating evidence suggested the important role of mitochondrial dysfunction in the pathogenesis of MC in both murine models of obesity and human obese patients [4,8,9]. Mitochondrial dysfunction, including impaired mitochondrial respiratory capacity, disturbed ATP generation, and accumulation of mitochondrial reactive oxygen species (mtROS), plays a rather pathogenic role in the onset of MC in obesity [10–12]. A clinical study demonstrated that obesity dominates mitochondrial defects in type 2 diabetes mellitus. Mitochondrial transmembrane potential and electron transport chain (ETC) activity were significantly decreased in obese-nondiabetic and obese-diabetic patients compared with those in control subjects, while no obvious change was observed in nonobese-diabetic patients [12]. In obesity, compromised mitochondrial respiratory capacity and increased mtROS production have been causally linked to impaired myocardial energetics [9,13]. In addition, mtROS elicited an increase of mitochondrial membrane permeability and even mitochondrial uncoupling, which finally impeded cardiac energy metabolism and reduced cardiac efficiency [9]. Nuclear factor erythroid 2-related factor 2 (Nrf2), a dominant transcription factor of cell defense against oxidative and xenobiotic stresses, regulates the downstream targets such as heme oxygenase 1 (HO-1, also known as HMOX1), NAD(P)H dehydrogenase quinone 1 (NQO1) and glutathione S-transferase pi 1 (GSTP1) [14–16]. It was reported that Nrf2/ARE signaling, as a crucial anti-oxidative stress machinery, was impaired in obesity [17]. Pharmacological Nrf2 activation has demonstrated protective outcomes on metabolic health [17,18]. However, naturally-occurring bioactive compounds which protects against obesity-associated MC remains scarce.

Isoginkgetin (IGK), a member of the biflavonoid family, is extracted from *Ginkgo biloba* and is a 3′,8″-dimerization product of its equivalent monoflavone residues, acacetin [19,20]. This 3′,8″-dimerization enhanced the antioxidant capacity of IGK compared with acacetin *in vitro* [20]. In a rodent model of cerebral ischemia/reperfusion injury, IGK treatment significantly counteracted cerebral infarction and neuron apoptosis [21]. However, the effects and molecular mechanism of IGK in heart disease remain elusive. In this study, we aimed to investigate the therapeutic effects and potential molecular mechanism of IGK in the treatment of obesity-induced MC.

2. Materials and methods

A detailed description of materials and methods is provided in the online Supplemental Materials and Methods. All data that support the findings of this study are available in the article and the online supplementary files.

2.1. Animal experimental design

The animal experiments were approved by the Animal Research Committee, Guangzhou Medical University (Guangzhou, China). All the experimental procedures were carried out according to the guidelines for the Care and Use of Laboratory Animals published by the United States National Institutes of Health (NIH Publication, revised 2011). Male C57BL/6 J mice (6–8 weeks old) were purchased from the Medical Experimental Animal Center of Guangdong Province. All the mice were raised in humidity- and temperature-controlled environment with a 12-h light/dark cycle, with food and water *ad libitum*.

Study 1: The mice were fed a high-fat diet (HFD, 60 kcal% fat, Research Diets D12492) or a standard chow diet (ND, 10% kcal fat) for 20 weeks and then subjected to IGK (0.5 mg/kg) or the vehicle by tail vein injection for another 4 weeks along with continuous HFD or ND feeding. The mice that did not gain 15% of body weight after 2 months' HFD consumption were excluded from subsequent analysis according to published literature [22]. There were no exclusions among mice fed a ND. A total of 48 mice were randomized into 4 groups: (i) ND + vehicle, (ii) ND + IGK, (iii) HFD + vehicle, (iv) HFD + IGK.

Study 2: A total of 32 mice fed on HFD were administered with 1 ×

10^{12} vg/mL of AAV9-cTnT-sh-Nrf2 or the scramble virus suspension diluted in 100 μL of saline via tail vein injection on week 19. One week later, the mice were treated with IGK (0.5 mg/kg) or the vehicle for another 4 weeks along with HFD feeding. The mice were randomized into 4 groups: (i) HFD + sh-NC, (ii) HFD + IGK + sh-NC, (iii) HFD + sh-Nrf2, (iv) HFD + IGK + sh-Nrf2.

Isoginkgetin (Cayman, US) was dissolved in dimethyl sulfoxide (DMSO) by the concentration of 50 mg/mL and stored at −80 °C. For tail vein injection, the stock solution was diluted in Tween-80 at a final concentration of 0.2 mg/mL.

2.2. Cell culture

Neonatal rat cardiomyocytes (NRCMs) were isolated from the Sprague-Dawley rats at postnatal day 1–3. After decapitation, hearts were removed and washed with pre-cooled Hank's balanced salt solution. The ventricles were cut to small pieces and suspended with 0.05% Trypsin solution (without EDTA) at 4 °C overnight. Ventricular tissues were digested by gentle shaking in 0.1% Type II Collagenase solutions at 37 °C for 45 min. The tissue lysate was filtered through 75 μm cell strainer mesh and repeated for 2 or 3 times until the tissue was digested completely. Cells were centrifuged at 1000 rpm for 5 min and resuspended in plating medium (DMEM, C11995500BT), added with 15% Fetal Bovine Serum (FBS) and plated in 100 mm dishes for 1 h to eliminate attached fibroblasts. Cardiomyocytes were collected and plated on 35 mm culture dishes at a density of 1×10^6 per dish. After 24 h, the cardiomyocytes were washed and plated in fresh medium for further experiments. The H9C2 cardiomyocytes were obtained from the American Type Culture Collection and cultured as described previously [23]. Both NRCMs and H9C2 cardiomyocytes were cultured in DMEM supplemented with 10% FBS and kept in the incubator with 5% CO_2 at 37 °C. To examine the effect of IGK on PA induced cardiomyocyte injury, the cells were treated with BSA-conjugated palmitic acid (PA, 400 μM) for 48 h with or without 10 μM IGK. All the experiments were repeated 3 times.

2.3. Statistical analysis

All data were analyzed with GraphPad Prism, version 8.0 (GraphPad Software) and expressed as means ± SD. Difference between two groups were analyzed using Student's *t*-test. Differences between multiple groups were analyzed using One-way ANOVA. $P < 0.05$ was considered as statistically significant.

3. Results

3.1. Isoginkgetin protects against diastolic dysfunction in the obese mice

To evaluate the effect of IGK on obesity-induced MC, a murine model of obesity was established by feeding the mice with high-fat diet (HFD, 60 kcal%) for 5 months (Supplementary material online, Fig. S1), which is an established model for investigating obesity-related disease including MC, with similar characteristics of human obesity [22,24–26]. We observed that HFD feeding induced obesity, mild hyperglycemia, and insulin resistance, all of which are characteristic of obesity. However, IGK treatment did not affect the rise of body weight and blood glucose level (Supplementary material online, Fig. S2).

To delineate the efficacy of IGK on MC, we conducted sequential transthoracic echocardiography assessments in the mice. Unexpectedly, we observed that left ventricular ejection fraction (LVEF) and left ventricular fraction shortening (LVFS) were preserved in both obese and non-obese mice up to 5 months of HFD feeding (Supplementary material online, Fig. S3). However, there is a significant decline of diastolic function in obese mice, as evidenced by the decrease of E/A ratio and a prolonged isovolumic relaxation time (IVRT) via Doppler echocardiography (Supplementary material online, Fig. S3), indicating the diastolic

dysfunction occurs in the mice fed on HFD for 5 months. Thereafter, 0.5 mg/kg of IGK was administered via tail vein injection for additional 4 weeks concurrent with HFD feeding (Supplementary material online, Fig. S1). Echocardiography assessment revealed no significant difference for either systolic or diastolic parameters in the mice fed with normal-diet (ND) treated with or without IGK (Fig. 1A–C, Supplementary material online, Table S1). As expected, the systolic parameters, including LVEF and LVFS, remain persistently preserved in the mice with HFD feeding. However, tissue Doppler ultrasonic measurements demonstrated a bigger ratio between mitral E wave and E′ wave (E/E′) in the HFD-fed mice, which is also indicative of diastolic dysfunction. Simultaneously, LV myocardial performance index (MPI) was impaired in the obese mice in comparison with that of control. Of note, IGK treatment leads to ameliorated LV diastolic dysfunction, as revealed by increased E/A ratio, shortened IVRT, declined E/E′ ratio and reduced MPI (Fig. 1D–H).

3.2. Isoginkgetin attenuates obesity-induced cardiac remodeling both in vivo and in vitro

Subsequently, we performed histological assessment to further explore the effect of IGK on cardiac remodeling in heart tissues. Cardiac hypertrophy was observed in the obese mice fed on HFD as evidenced by higher ratio of heart weight to tibia length (HW/TL) (Fig. 2A), increased cross-sectional area of cardiomyocytes (Fig. 2B and C), and increased mRNA level of established pro-hypertrophic genes, such as natriuretic peptide type A (*Nppa*), natriuretic peptide B (*Nppb*) (Fig. 2D and E). Notably, these changes were significantly alleviated in the obese mice treated with IGK (Fig. 2A–E). In addition, Masson's trichrome staining showed that fibrosis was significantly alleviated in the IGK treated obese mice, compared with those treated with vehicle (Fig. 2F and G). Together, these data suggests that IGK treatment protects against obesity-induced adverse cardiac remodeling in the HFD-fed mice.

Pathological cardiomyocyte hypertrophy is one of the hallmarks of adverse cardiac remodeling [27]. We isolated neonatal rat cardiomyocytes and further examined the effect of IGK on cardiac
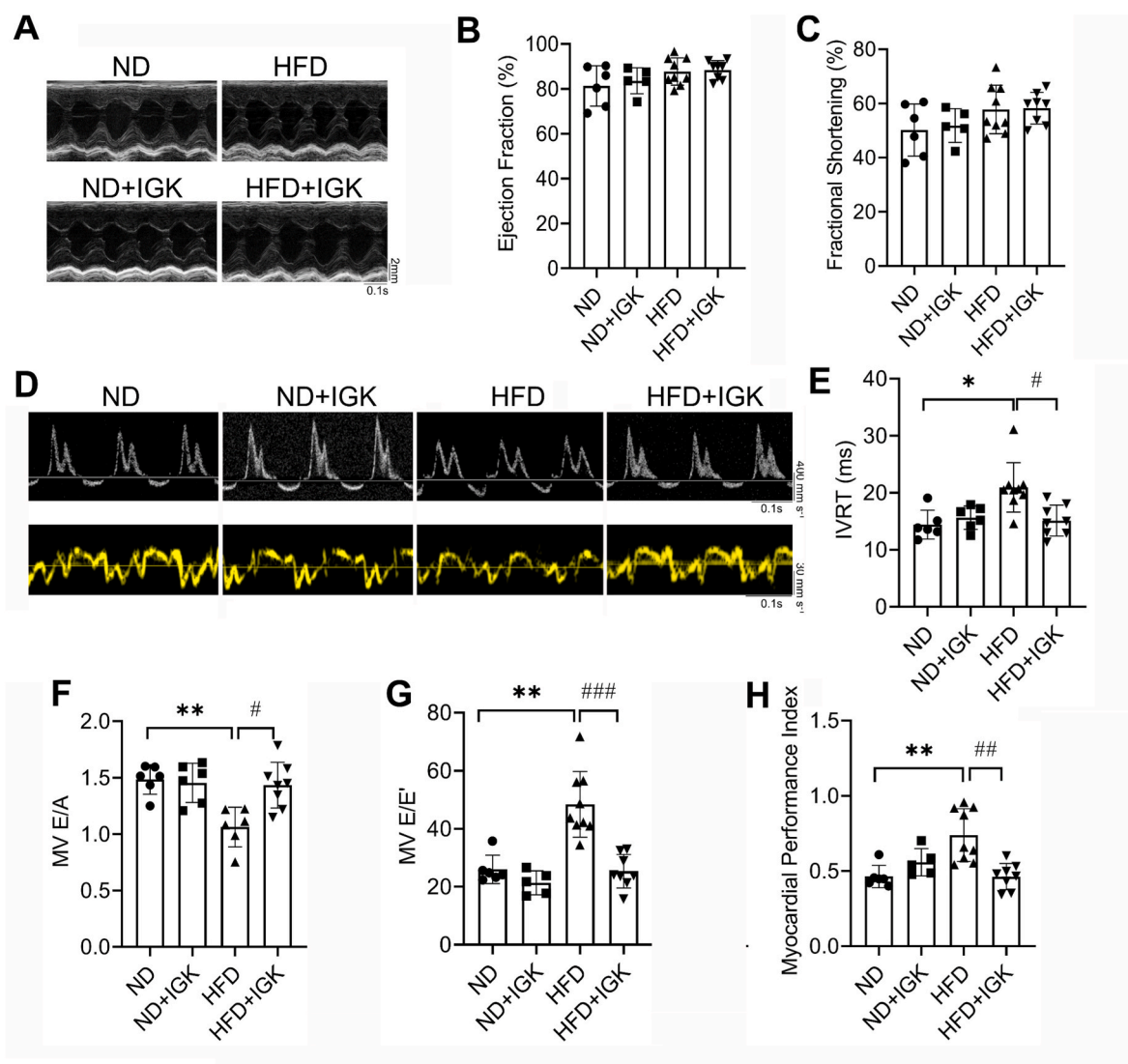

Fig. 1. Isoginkgetin protects against diastolic dysfunction in the obese mice. (A) Representative images of M-mode echocardiography of left ventricle. (B) Left ventricular ejection fraction (LVEF) of different groups ($n = 6, 5, 9$ and 8, respectively). (C) Left ventricular fractional shortening (LVFS) of different groups ($n = 6, 5, 9$ and 8, respectively). (D) Representative images of pulsed-wave Doppler (upper panel) and tissue Doppler (lower panel). (E) Isovolumic relaxation time (IVRT) of different groups ($n = 6, 6, 9$ and 8, respectively). (F) E/A ratio (MV E/A) of different groups ($n = 6, 6, 6$ and 8, respectively). (G) E/E′ ratio (MV E/E′) of different groups ($n = 6, 5, 9$ and 8, respectively). (H) Myocardial performance index of different groups ($n = 6, 5, 9$ and 8, respectively). Data were shown as mean ± SD. $*P < 0.05$, $**P < 0.01$, *vs.* ND group; $^{\#}P < 0.05$, $^{\#\#}P < 0.01$, $^{\#\#\#}P < 0.001$ *vs.* HFD group. Statistical analysis was carried out by a one-way ANOVA test.
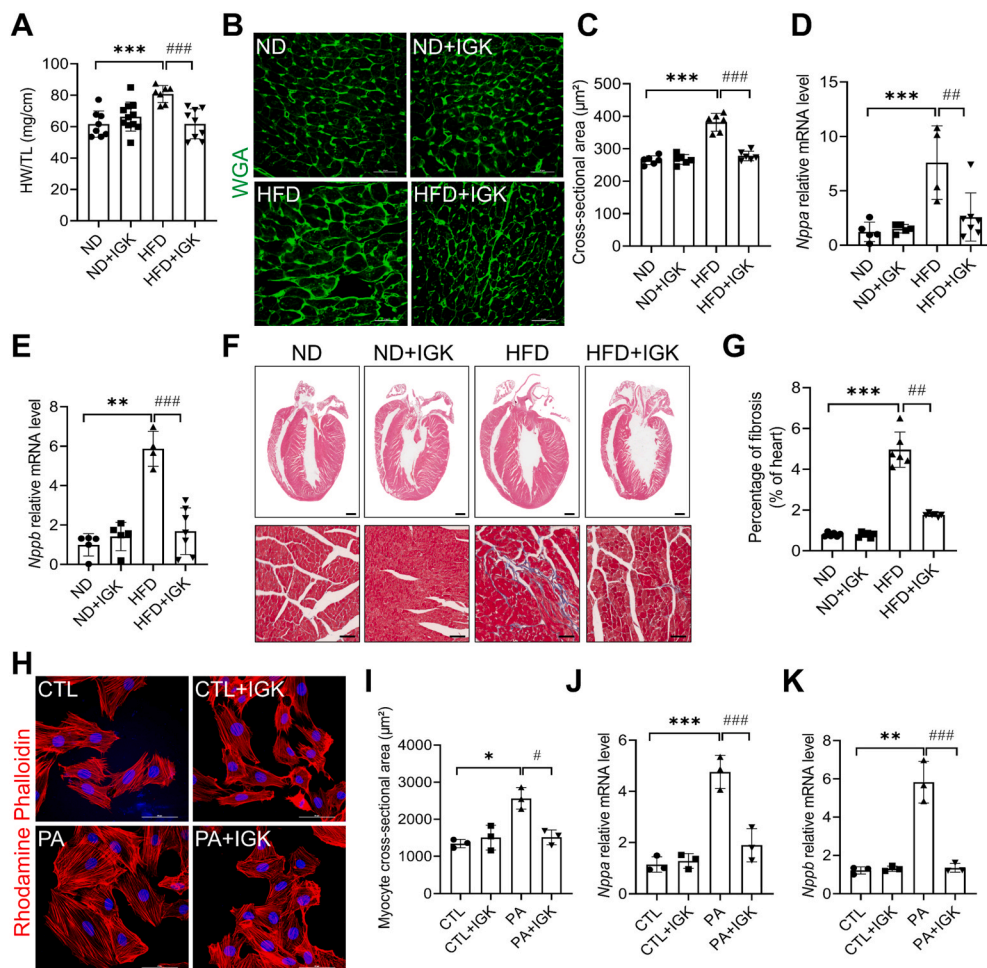
Fig. 2. Isoginkgetin attenuates pathological cardiac remodeling in obese mice. (A) Ratio of heart weight to tibia length (HW/TL), $n = 8, 11, 7, 9$ mice respectively. (B) Representative images of left ventricular cardiomyocytes cross-sectional area depicted by Wheat germ agglutinin staining (WGA). Scale bars: 50 μm. (C) WGA quantification of cardiomyocyte cross-sectional area ($n = 6$ mice per group). (D–E) Natriuretic peptide A (*Nppa*) and natriuretic peptide B (*Nppb*) mRNA ($n = 5, 5, 4, 7$ mice per group). (F) Upper: representative hematoxylin and eosin (H&E) stained sections of left ventricles in mice. Scale bars: 1 mm. Lower: representative Masson's Trichrome stained sections of left ventricles in mice. Scale bars: 100 μm. (G) Quantification of fibrosis area of left ventricles in mice, $n = 6$ mice per group. (H) Representative images of NRCMs stained by rhodamine phalloidin and 4′,6′-diamidino-2-phenylindole (DAPI). Scale bars: 50 μm. (I) Quantification of cell cross-sectional area from 3 independent experiments. (J and K) The mRNA expression level of *Nppa* and *Nppb* in the NRCMs (3 independent experiments). Data were shown as mean ± SD, *$P < 0.05$, **$P < 0.01$, ***$P < 0.001$ *vs.* ND or CTL group; #$P < 0.05$, ##$P < 0.01$, ###$P < 0.001$ *vs.* HFD or PA group. Data were analyzed by one-way ANOVA.

hypertrophy *in vitro* with the pathological stimuli of palmitic acid. Rhodamine phalloidin staining showed that PA could significantly increase the cardiomyocyte cross-sectional area and the expression of

pro-hypertrophic genes, such as *Nppa* and *Nppb*, whereas both of which were attenuated with IGK treatment (Fig. 2H–K).

Given that excessive lipid accumulation drives oxidative stress and
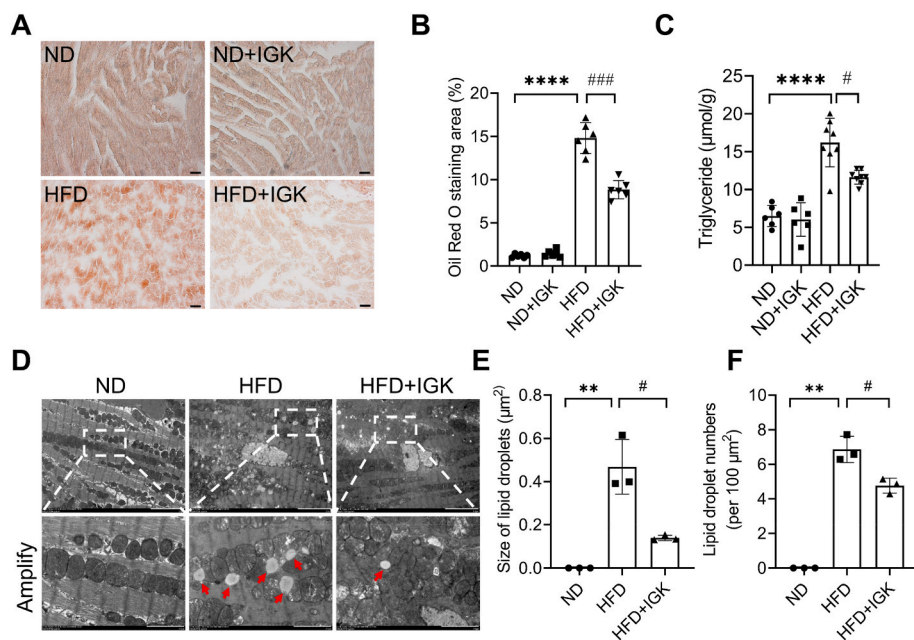

Fig. 3. Isoginkgetin attenuates intramyocardial lipid accumulation in the obese mice. (A) Representative Oil Red O staining of cardiac sections. Scale bar: 50 μm. (B) Quantification of relative Oil Red O positive area ($n = 6$ per group). (C) Measurement of triglyceride content in the heart tissue of the mice. ($n = 6, 6, 8, 8$ mice respectively) (D) TEM images of the heart tissue. Scale bar: 5 μm (upper) or 2 μm (lower). Red arrow indicates lipid droplets. (E) Quantification of the size of lipid droplets (expressed as μm²). $n = 3$ different images. (F) Quantification of the number of lipid droplets (expressed per 100 μm²). $n = 3$ different images. Data were shown as mean ± SD, **$P < 0.01$, ****$P < 0.0001$ *vs.* ND group; #$P < 0.05$, ###$P < 0.001$ *vs.* HFD group. Data were analyzed by one-way ANOVA. (For interpretation of the references to colour in this figure legend, the reader is referred to the Web version of this article.)

cardiomyocyte damage in metabolic cardiomyopathy [28], we performed Oil Red O staining and transmission electron microscopy (TEM) assessment on the myocardial sections. We observed that there was no obvious lipid droplets (LDs) accumulation in the mice fed on normal diet with either IGK or vehicle treatment. However, the intramyocardial LDs accumulation were remarkably increased in the mice fed on HFD (Fig. 3A and B), which was attenuated by IGK treatment. Additionally, direct measurement of cardiac lipid contents demonstrated that triglycerides was decreased in the IGK-treated obese mice as compared with that of ones treated with vehicle (Fig. 3C). Moreover, TEM demonstrated that LDs accumulation were significantly decreased in the obese mice with IGK treatment (Fig. 3D–F).

Together, these data demonstrated that IGK mitigated intramyocardial lipid accumulation and cardiac remodeling in the obese mice.

3.3. Isoginkgetin activates Nrf2/ARE signaling and protects against mitochondrial dysfunction in the obese mice

To identify the molecular mechanism whereby IGK confers antihypertrophic and anti-fibrotic effects in the obese mice, RNA-sequencing of heart samples from the obese mice treated with or without IGK was performed. In total, 377 genes were significantly upregulated, and 385 genes were significantly downregulated in the heart tissues of the IGK-treated obese mice, compared with that of vehicle-treated mice ($P < 0.05$) (Fig. 4A). Pathway analysis of the differentially expressed genes indicated that Nrf2 signaling pathway was enriched in the upregulated genes in IGK-treated heart tissues (Fig. 4B). We then confirmed that the expression of Nrf2 and its downstream genes, such as HO-1, NQO1 and GSTP1 were upregulated with IGK treatment (Fig. 4C and D). Among these known Nrf2 target genes, the expression level of HO-1 was the most significant, confirming that IGK treatment activated Nrf2 defense in the HFD-fed mice. In addition, a burst of ROS production in the heart was observed in HFD-fed mice, which was significantly alleviated by IGK treatment (Fig. 4E and F). Moreover, mice treated with IGK displayed less mtROS production compared to the vehicle control. IGK administration did not alter mtROS production in the mice fed on ND (Fig. 4G and H). It was reported that Nrf2 mediated antioxidant defense via targeting on HO-1 and NQO1, or maladaptive pathological consequence via targeting on angiotensinogen (Agt) and Kruppel-like factor (Klf) 9 [29,30]. As shown in Supplementary Fig. S4, the mRNA level of Agt and Klf9 was increased in the heart of HFD fed mice, however, which was not changed with IGK treatment in the obese heart. These data indicate that IGK treatment has minimal effect on Nrf2-operated pathological response in the heart.

It was reported that Nrf2 accelerates mitochondrial fatty acid oxidation [31,32]. Of note, KEGG pathway analysis showed that mitochondrial complex assembly, mitochondrial complex III and I assembly, oxidative phosphorylation along with Nrf2 signaling were enriched in IGK-treated obese mice heart (Fig. 4B and Supplementary material online, Table S2). Therefore, we assessed the activity of mitochondrial respiratory electron transport chain (ETC). The protein expression of mitochondrial ETC of CI–V subunits was decreased in the hearts of the mice fed on HFD, whereas which were markedly upregulated in the obese mice treated with IGK (Fig. 4I). The protection on mitochondrial ETC capacity mediated by IGK treatment was also demonstrated by the increase of ATP content compared with that of vehicle treated hearts (Fig. 4J). Impaired oxidative phosphorylation is certainly associated with decreased mitochondrial bioenergetics, which contributes to mitochondrial abnormalities in the setting of obesity [33]. So, we further observed mitochondrial ultrastructure using transmission electron microscopy. Numerous swollen mitochondria, reduced matrix density and cristae disorganization were observed in the heart of obese mice, whereas which was rejuvenated by IGK treatment (Fig. 4K and L).

3.4. Isoginkgetin promotes Nrf2 nuclear translocation and mitigates PA-induced mitochondrial dysfunction in cardiomyocytes

To further consolidate the effect of IGK on Nrf2 signaling, the primarily isolated neonatal cardiomyocytes were treated with IGK *in vitro*. IGK treatment increased the total protein level of Nrf2 and its downstream targets including HO-1, NQO1 and GSTP1 (Supplementary material online, Figs. S5A and B) in the cardiomyocytes under the basal condition. Furthermore, IGK treatment promoted Nrf2 translocation to the nucleus with a peak level between 6 h and 12 h (Supplementary material online, Figs. S5C and D). Moreover, the nuclear translocation of Nrf2 was confirmed by confocal microscopic analysis (Supplementary material online, Figs. S5E and F).

Next, we examined the unique effect of IGK on Nrf2 signaling under the condition of PA challenge. Similarly, IGK led to an increase of total protein level of Nrf2 and its downstream targets (Fig. 5A), and also promoted Nrf2 nuclear translocation after PA stimulation (Fig. 5B–D). Consistent with what we found *in vivo*, PA-induced mitochondrial superoxide production was significantly mitigated by IGK treatment (Fig. 5E and F). Moreover, JC-1 staining demonstrated that PA-treated cardiomyocyte exhibited a significant decrease in the ratio of aggregates/monomers fluorescence intensity, indicating the collapse of mitochondrial potential ($\Delta\Psi m$); however, this effect was alleviated by IGK treatment (Fig. 5G and H). Furthermore, we used a Seahorse extracellular flux analyzer to examine the mitochondrial respiratory capacity in the isolated neonatal cardiomyocytes. The result demonstrated that both the maximal and spare respiratory capacity were decreased in the PA-challenged cardiomyocytes, whereas these defects were partially amended by IGK treatment (Fig. 5I and J). IGK treatment elicited not discernible change under the basal condition. These results confirmed that IGK activated Nrf2/ARE anti-oxidative stress signaling pathway and restored mitochondrial respiratory capacity *in vitro*.

3.5. Molecular docking study revealed the binding of isoginkgetin with Nrf2

To gain further structural insight into the mechanism whereby Nrf2/ARE signaling pathway was activated by IGK, we used Discovery Studio 3.1 software to perform a molecular docking simulation, with an aim to predicting whether there is direct interaction between IGK and Nrf2. As shown in Fig. 6A–C, the binging mode of IGK and crystal structure of Keap1/Nrf2 complex (PDB: $1 \times 2R$) showed that IGK enters the pocket of Keap1/Nrf2 complex by 6 hydrogen bonds, which turned out to be Arg-415 (1.7 Å), Ser-602 (2.0 Å), GLN-530 (2.2 Å), ARG-380 (2.4 Å), SER-508 (2.5 Å) and ASN-382 (2.5 Å). To further evaluate the structural stability of the complex between IGK and Nrf2, the time evolution of weighted root-mean-square deviations (RMSDs) was conducted. The steady RMSDs of the protein backbone structures demonstrated that the combination of IGK and Nrf2 has a good equilibrium (Fig. 6D and E). Consistent with our docking results, these data extracted from the 100 ns of molecular dynamics simulations, the H-bonds linked to Arg-415, Ser-602, GLN-530, ARG-380, and SER-508 residues were preserved. Taken together, these data indicated that IGK can potentially bind within the Nrf2 pocket, creating a stable complex of relatively high affinity.

3.6. Isoginkgetin activates Nrf2 signaling via inhibiting ubiquitin dependent proteasomal degradation

To dissect the direct molecular mechanism whereby IGK regulates Nrf2, the cardiomyocytes were exposed to IGK with or without PA stimulation. As described above, IGK treatment promoted the protein expression level of Nrf2 and downstream AREs-containing proteins (HO-1, NQO1 and GSTP1) (Supplementary material online, Figure S5 A-B). Unexpectedly, mRNA level of Nrf2 (Fig. 7A) did not differ between the treatment of IGK and that of vehicle either in the absence or presence of PA challenge, suggesting that IGK regulates Nrf2 at the post-
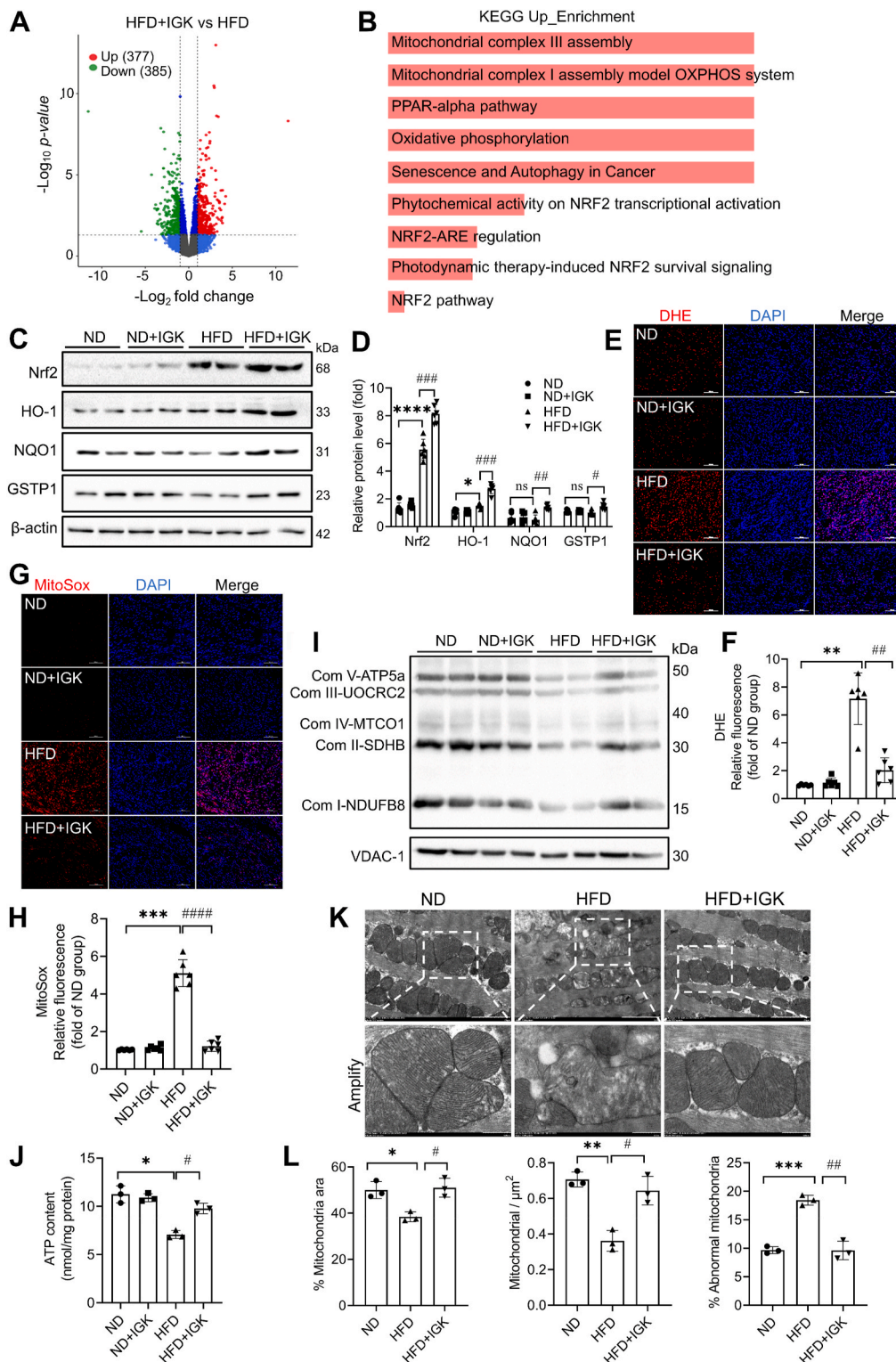
Fig. 4. Isoginkgetin activates Nrf2/ARE signaling and protects against mitochondrial abnormalities in the obese mice. (A) Volcano plot shows the differentially expressed genes in the obese heart with IGK treatment compared with that of vehicle treatment. (B) Kyoto Encyclopedia of Genes and Genomes (KEGG) pathway analysis of the differentially upregulated genes in IGK-treated obese mice. (C–D) Myocardial protein Nrf2, HO-1, NQO1 and GSTP1 were determined by Western blot analysis and quantified below ($n = 6$ per group). (E–F) Representative images and analysis of dihydroethidium (DHE) staining of cardiac section in mice. Scale bars: 100 μm, $n = 6$ per group. (G–H) Representative images and analysis of MitoSox staining of cardiac section in mice. Scale bars: 100 μm, $n = 6$ per group. (I) Representative immunoblotting images of ETC complex subunits from indicated groups. (J) ATP content in the heart tissues from indicated groups. ($n = 3$ for each group). (K) Representative transmission electron microscopy images of heart tissue from indicated groups. Scale bars: 2 μm (upper) or 500 nm (lower). (L) Quantification of mitochondria-related parameters. % Mitochondria area refers to the ratio of mitochondrial area to image area; mitochondrial/μm^2 refers to mitochondrial density; % abnormal mitochondria refers to the ratio of abnormal mitochondria in hearts. ($n = 3$ for each group). Data were shown as mean ± SD, *$P < 0.05$, **$P < 0.01$, ***$P < 0.001$, ****$P < 0.0001$ vs. ND group; #$P < 0.05$, ##$P < 0.01$, ###$P < 0.001$, ####$P < 0.0001$ vs. HFD group. Data were analyzed by one-way ANOVA.
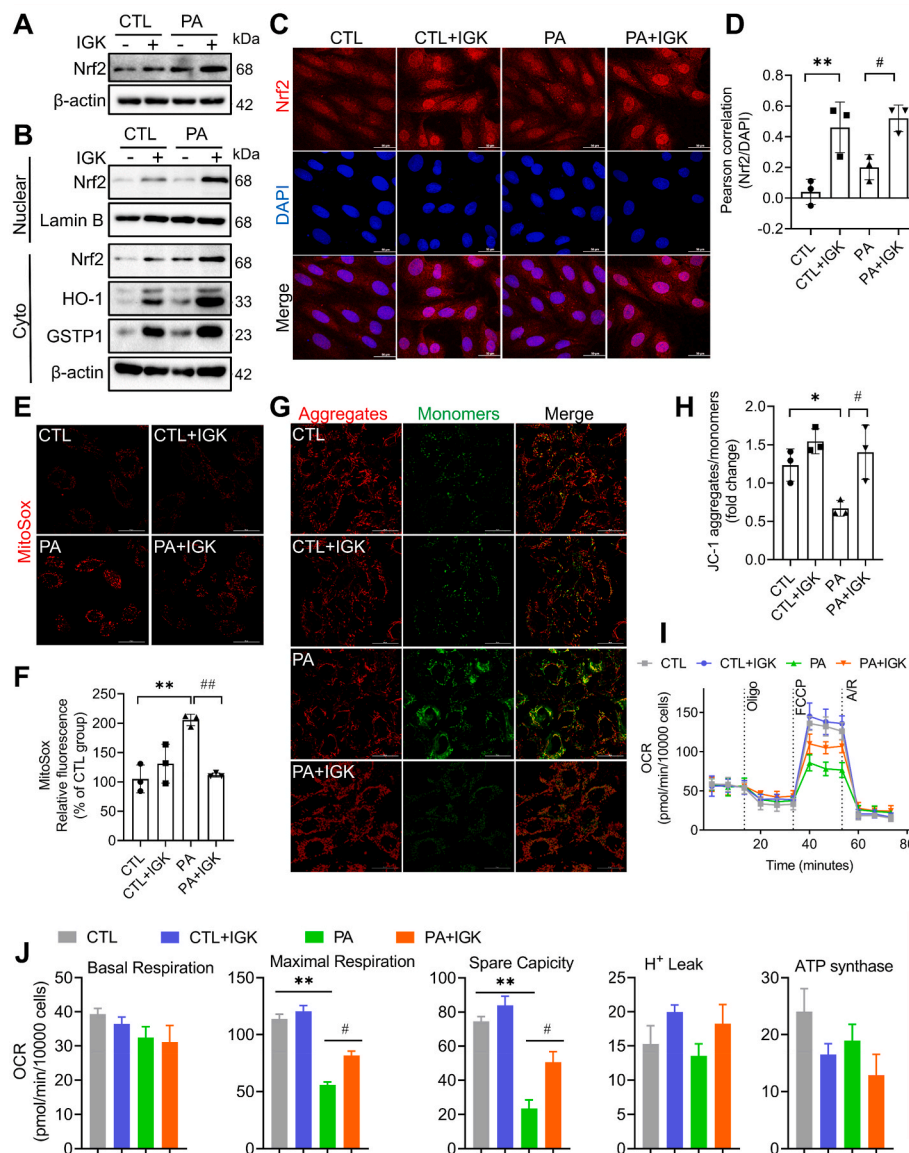
Fig. 5. Isoginkgetin promotes Nrf2 nuclear translocation and mitigated PA-induced oxidative stress in cardiomyocytes. (A) Effect of IGK treatment on Nrf2 protein level in palmitic acid-treated cardiomyocytes were detected by immunoblotting. (B) After the NRCMs were treated with vehicle or IGK in the presence or absence of palmitic acid as above, Nrf2 translocation was detected by immunoblotting by analyzing the level of Nrf2 in the nuclear and cytosolic fraction. (C) Representative immunofluorescent images of Nrf2 immunofluorescence in the NRCMs treated with or without IGK in the presence or absence of PA. Scale bars: 50 μm. (D) Quantification of colocalization of Nrf2 and nuclei. $n = 3$ independent experiments. (E and F) Representative images and analysis of MitoSox in the neonatal cardiomyocytes. Scale bars: 50 μm, $n = 3$ independent experiments. (G and H) Representative images and quantified analysis of JC-1 staining in NRCMs. Scale bars: 50 μm, $n = 3$ independent experiments. (I and J) Mitochondrial oxidative respiration of the neonatal cardiomyocytes with IGK or vehicle in the presence or absence of PA as assessed by measurement of cellular oxygen consumption rate (OCR). Data were presented as mean ± SD. $n = 3$ independent experiments. $*P < 0.05$, $**P < 0.01$ *vs.* CTL group; $^{\#}P < 0.05$, $^{\#\#}P < 0.01$ *vs.* PA group. Data were analyzed by one-way ANOVA.
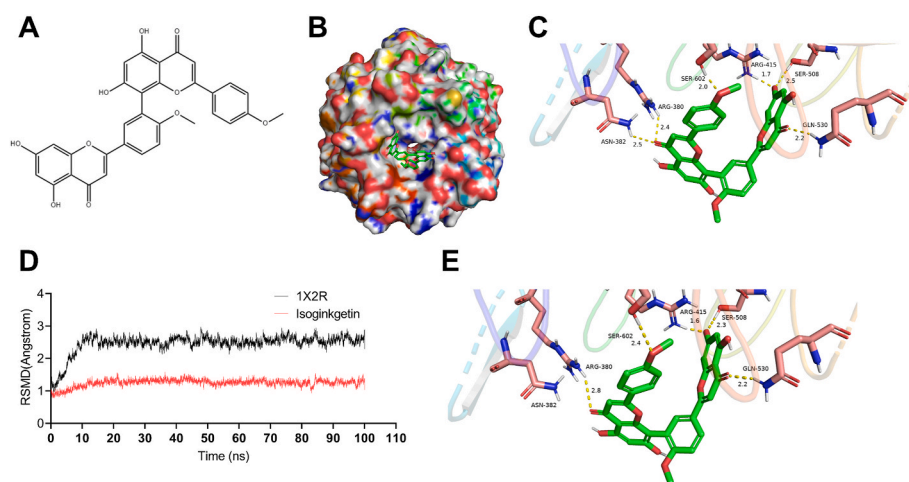

Fig. 6. Molecular modeling and docking analysis reveal the binding of IGK with Nrf2. (A) The chemical structure of IGK. (B) Surface representation of the crystal structure of Keap1 (PDB ID: 1X2R) in complex with IGK (green). (C) Front view of docking mode of IGK in the binding pocket of 1X2R. H-bond (yellow): Arg-415 (1.7 Å), Ser- 602 (2.0 Å), GLN-530 (2.2 Å), ARG-380 (2.4 Å), SER-508 (2.5 Å) and ASN-382 (2.5 Å). (D) RMSDs values investigation through MD simulations. (E) The last frame was extracted as a representative. (For interpretation of the references to colour in this figure legend, the reader is referred to the Web version of this article.)
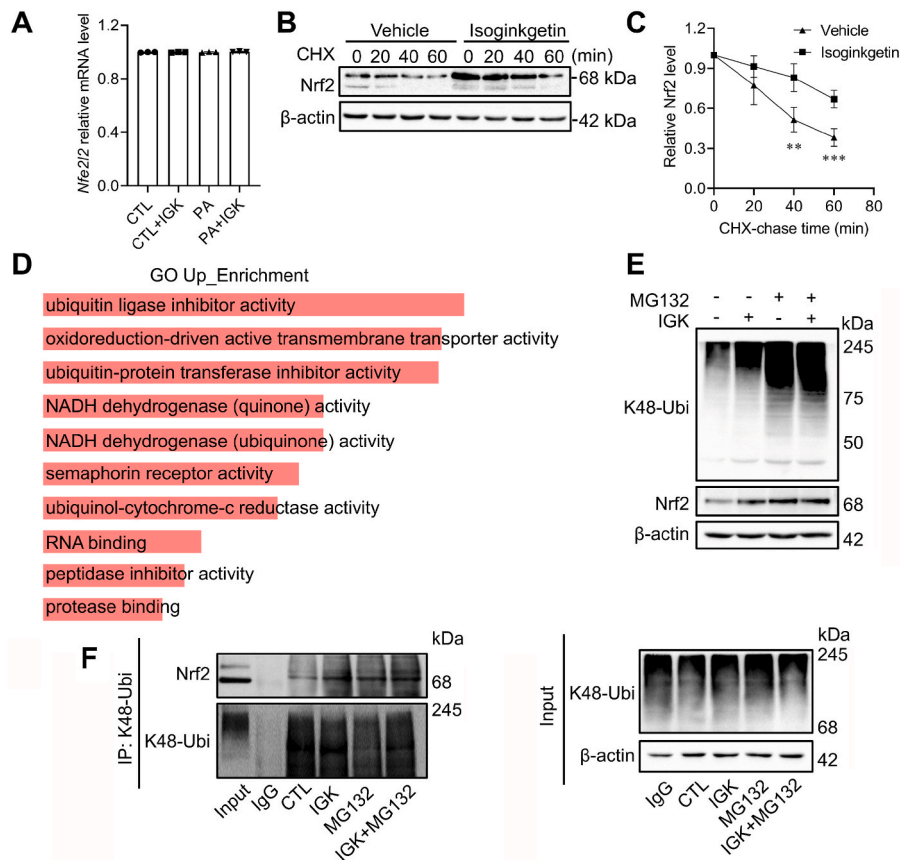
Fig. 7. Isoginkgetin activates Nrf2 signaling pathway via inhibiting ubiquitin dependent proteasomal degradation. (A) The neonatal cardiomyocytes were stimulated with PA (400 μM) for 24 h with IGK (10 μM) or the vehicle. Then the mRNA expression of Nrf2 was detected by qPCR, $n = 3$. (B and C) The neonatal cardiomyocytes were treated with IGK (10 μM) for 1 h followed by incubation with CHX (300 μM) for indicated times respectively. The expression of Nrf2 was determined by Western blot, $n = 3$. (D) Gene ontology analysis of differentially upregulated genes in IGK-treated obese mice by RNA-seq. (E) The neonatal cardiomyocytes were treated with IGK (10 μM) or the vehicle in the presence or absence of MG132 (10 μM) for 2 h. Representative images of immunoblot analysis of total Nrf2 protein levels and total K48 ubiquitinated proteins levels. $n = 3$ independent experiments. (F) The neonatal cardiomyocytes were treated with IGK (10 μM) or the vehicle in the presence or absence of MG132 (10 μM) for 2 h. Representative images of immunoprecipitation assay showing that Nrf2 interacted with ubiquitin-K48 in cells. The cell lysates were immunoprecipitated with ubiquitin-K48 antibody, and then analyzed by immunoblotting. Input was used as a positive control and IgG was used as a negative control. Data were presented as mean ± SD, $**P < 0.01$, $***P < 0.001$ *vs.* Vehicle group. Data were analyzed by Student's *t*-test.

translational level. To explore whether accumulation of Nrf2 protein was attributable to an increase of its stability, the half-life of Nrf2 in cardiomyocytes was measured. By performing cycloheximide (CHX) chasing experiments, the cardiomyocytes co-treated with IGK and CHX exhibited a delayed Nrf2 degradation curve as compared with those treated with CHX alone, indicating that the half-life of Nrf2 was extended in the presence of IGK (Fig. 7B and C). Of note, Gene Ontology enrichment analysis demonstrated that ubiquitin ligase inhibitor activity is among the top enriched pathways in the heart of IGK treated mice (Fig. 7D and Supplementary material online, Table S3). Nrf2 degradation is predominantly mediated by protein polyubiquitylation, which targets it for proteasomal degradation in a Keap1-dependent or independent manner [34,35]. Unexpectedly, IGK did not alter the protein expression of Keap1 (Supplementary material online, Fig. S6). We further examine whether IGK affects the degradation of Nrf2 by the ubiquitin-proteasome system. The cardiomyocytes were treated with IGK or the vehicle in the presence or absence of MG132. Intriguingly, IGK treatment results in an accumulation of both total ubiquitinated proteins and K48-linked ubiquitinated proteins, similar to MG132, a well-established proteasome inhibitor (Fig. 7E, Supplementary material online, Fig. S7), indicating that IGK increases the protein level of Nrf2 mainly via inhibiting its proteasomal degradation.

To further confirm that IGK treatment regulates endogenous ubiquitin-proteasome mediated Nrf2 degradation, the whole-cell lysates were immunoprecipitated with anti-K48-ubiquitin. The precipitates analysis demonstrated that increased Nrf2 was conjugated to K48-ubiquitin to form polyubiquitinated species in response to IGK treatment, and this response was similar with MG132 cotreatment (Fig. 7F). Overall, these data suggest that IGK increases protein level of Nrf2 by inhibiting its proteasomal degradation.

3.7. Genetic silencing of Nrf2 blunts the myocardial protective effect of isoginkgetin against PA challenge

Considering that IGK treatment activated Nrf2/ARE signaling pathway, we reasoned whether the cardioprotective effects afforded by IGK against myocardial dysfunction was attributed to Nrf2 upregulation. To test this hypothesis, Nrf2 was silenced by siRNA in the cardiomyocytes. The knockdown efficiency of siNrf2 was confirmed by immunoblotting assays (Fig. 8A, Supplementary material online, Fig. S8). Rhodamine staining and mRNA level of pro-hypertrophic genes *Nppa* and *Nppb* showed that protective effects of IGK treatment against cardiomyocyte hypertrophy were blunted by siNrf2 treatment (Fig. 8B–E). Furthermore, IGK-mediated suppressive effects on mtROS production were also ablated by siNrf2 treatment (Fig. 8F and G). In addition, siNrf2 also abrogated IGK-mediated mitochondrial membrane potential polarization (Fig. 8H and I). Collectively, these data illustrated that IGK protected against cardiomyocyte damage and mitochondrial dysfunction at least partially via Nrf2/ARE signaling pathway.

3.8. Nrf2 knockdown dampens the protective effect of isoginkgetin in obesity-induced cardiac dysfunction and mitochondrial defects

In order to demonstrate whether the cardioprotective effects of IGK depend on Nrf2/ARE signaling activation *in vivo*, we generated a cardiac-specific Nrf2-knockdown mice by tail vein injection of AAV9-cTnT-sh-Nrf2. The experimental design was shown in Supplementary material online, Fig. S9. Immunoblotting assay confirmed that Nrf2 and its downstream proteins (HO-1 and GSTP1) were downregulated efficiently in the heart tissues of the mice injected with AAV9-cTnT-sh-Nrf2 (Fig. 9A and B). Notably, the specificity of Nrf2 knockdown in cardiomyocytes from AAV9-cTnT-sh-Nrf2 treated mice was confirmed by confocal microscopy (Supplementary material online, Fig. S10). Also,
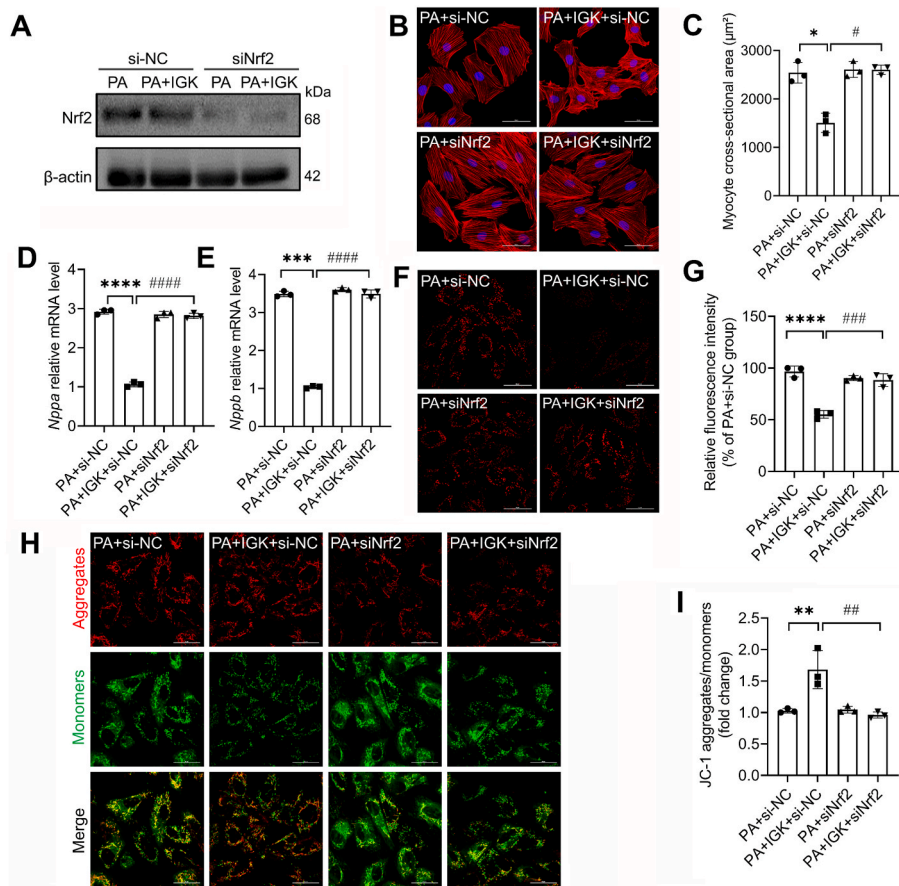
Fig. 8. Genetic knockdown of Nrf2 blunts the protective effect of IGK on cardiomyocyte hypertrophy, ROS production and mitochondrial injury. (A) Representative images of Nrf2 protein expression of indicated groups. (B) Representative images of neonatal cardiomyocytes pretreated with siNrf2 or si-NC for 48 h following PA stimulation with or without IGK treatment. Rhodamine phalloidin staining was performed to measure cell surface area. Scale bars: 50 μm. (C) Quantification of cell area. (D and E) mRNA expression of *Nppa* and *Nppb* in neonatal cardiomyocytes. (F) Representative images of neonatal cardiomyocytes staining with MitoSox. Scale bars: 50 μm. (G) Quantification of mitochondrial reactive oxygen species levels measured by relative fluorescence intensity. (H) Representative images of JC-1 staining in neonatal cardiomyocytes. Scale bars: 50 μm. (I) Quantification of JC-1 staining based on the measurement of relative fluorescence intensity. Data were presented as mean ± SD, *$P < 0.05$, **$P < 0.01$, ***$P < 0.001$, ****$P < 0.0001$ *vs.* PA + si-NC group; #$P < 0.05$, ##$P < 0.01$, ###$P < 0.001$, ####$P < 0.0001$ *vs.* PA + IGK + si-NC group. Data were analyzed by one-way ANOVA, $n = 3$ independent experiments.

echocardiographic assessment demonstrated that the protective effect of IGK against obesity-induced diastolic dysfunction was mitigated by Nrf2 knockdown (Fig. 9C–F). Moreover, Nrf2 knockdown also abrogated the beneficial effect of IGK on cardiac remodeling, as revealed by increased ratio of HW/TL, cross-sectional area of cardiomyocytes and fibrosis area (Fig. 9G–K). Furthermore, the enhancement of mitochondrial ETC by IGK treatment in the obese heart was compromised with Nrf2 knockdown (Figure 9L). Consistently, Nrf2 knockdown blunted the protective effect of IGK as evidence by the accumulation of ROS (Figure 9M).

Taken together, these data confirmed that IGK treatment contributes towards protection against obesity-associated MC through Nrf2/ARE signaling pathway.

3.9. Safety profile of isoginkgetin in mice

To further evaluate the safety profile of IGK, we performed blood biochemical analysis and histological assessment of major organs/tissues. We first evaluate the possibility whether IGK treatment had toxicity on the liver, the major metabolic organ in humans. Plasma levels of alanine aminotransferase (ALT) and aspartate aminotransferase (AST), two well-established markers of hepatic injury, were not altered by IGK treatment (Supplementary material online, Figs. S11A and B). Consistently, hepatic histology (H&E staining) analysis, did not display any signs of hepatocyte injury or necrosis of hepatic cord (Supplementary material online, Fig. S10C). In addition, no toxicity was observed in the kidney and spleen by H&E staining (Supplementary material online, Fig. S10C). Furthermore, lipid and blood glucose levels showed no significant difference in the mice treated with or without IGK (Supplementary material online, Figs. S11D and E, Fig. S2B).

4. Discussion

With the dramatic rise of obesity worldwide, both the morbidity and mortality of MC are increasing, with no effective therapies being available [2,36]. In the present study, we demonstrated that IGK treatment protects against obesity-induced cardiomyopathy both *in vivo* and *in vitro*. The salient findings of the present study are: (i) IGK protected against obesity-induced cardiomyopathy, including improved diastolic function and attenuated adverse cardiac remodeling. (ii) IGK activated Nrf2/ARE signaling and improved mitochondrial respiratory ETC capacity as evidenced by transcriptomic profiling and biological validation. (iii) Structurally, IGK entered the pocket of Keap1/Nrf2 complex with 6 H-bond bindings and promoted its nuclear translocation, which triggers the expression of Nrf2 downstream genes activation. (iv) The cardioprotective effects of IGK treatment were attributable, at least partially, to Nrf2/ARE signaling activation, which alleviates oxidative stress and mitochondrial defects. (v) Mechanistically, IGK promotes Nrf2 stability via inhibiting the proteasome-dependent degradation of Nrf2. Collectively, our data identify and validate IGK as a novel bioactive constituent from *Ginkgo Biloba*, to alleviate the excess ROS production and potentially protect against obesity-induced cardiomyopathy.

Prevalence of obesity is currently escalating worldwide, and it is closely associated with MC [37]. Of note, no effective therapy is available to treat obesity-associated MC and its complications. Isoginkgetin, a biflavone from *Ginkgo Biloba*, was identified as an inhibitor of RNA splicing [38] and was reported to possess multiple protective effects including anti-inflammation [21,39,40], anti-oxidative stress [20] and anti-tumorigenic activities [41,42]. Our data demonstrated for the first time that IGK ameliorated diastolic dysfunction, cardiac hypertrophy
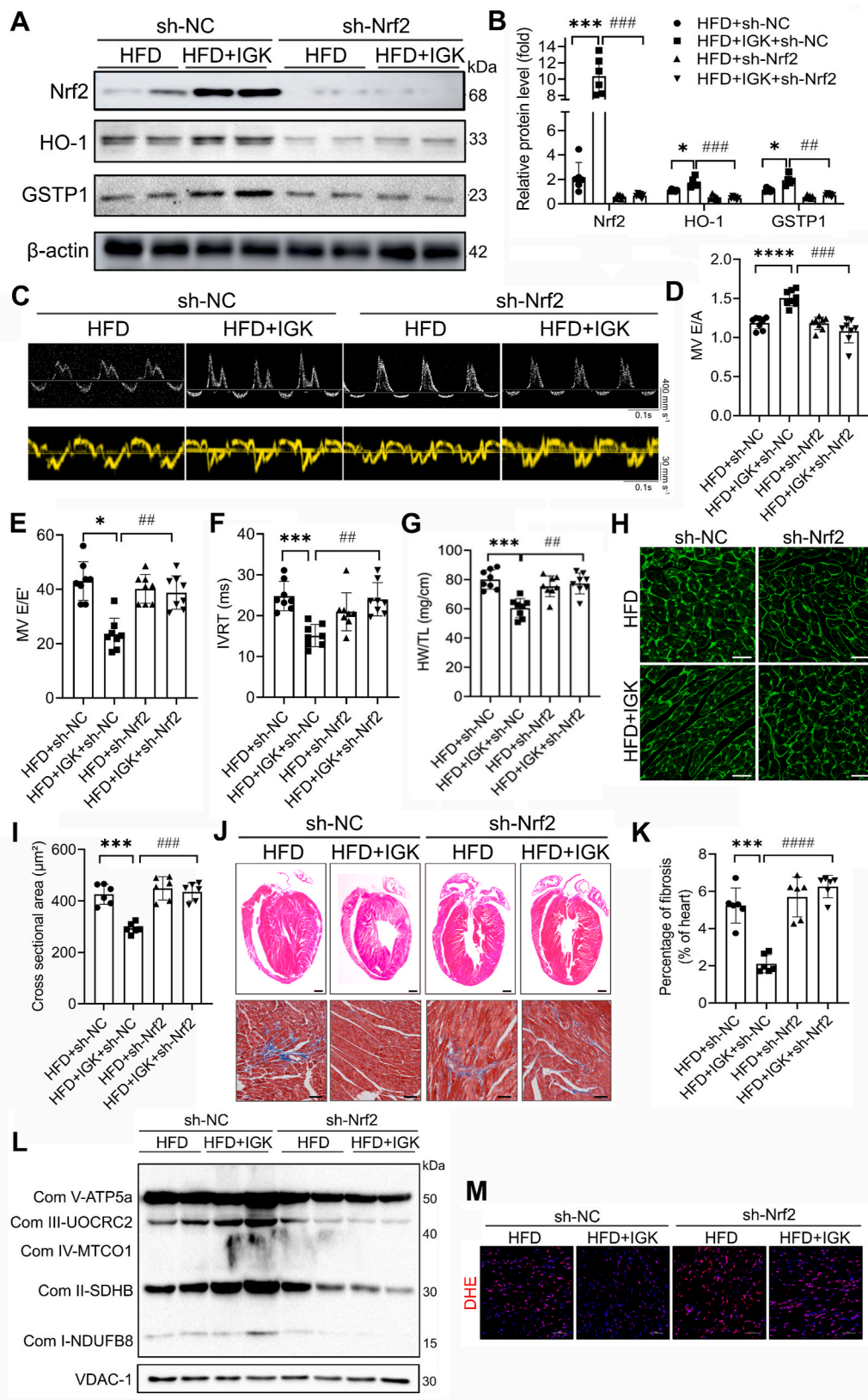
Fig. 9. Genetic knockdown of Nrf2 blunts the cardioprotective effect of IGK in obese mice. (A) Representative image and (B) quantification of Immunoblotting assay to determine the myocardial protein Nrf2, HO-1, NQO1 and GSTP1 ($n = 6$ per group). (C) Representative images of pulsed-wave Doppler (upper panel) and tissue Doppler (lower panel), $n = 8$ per group. (D) Quantification of E/A ratio, (E) E/E′ ratio, (F) IVRT, (G) Ratio of HW/TL, $n = 8$ per group. (H) Representative images of left ventricular cardiomyocytes cross-sectional area depicted by WGA staining. Scale bars: 50 μm. (I) WGA quantification of cardiomyocyte cross-sectional area ($n = 6$ mice per group). (J) Upper: representative H&E-stained sections of left ventricles in mice. Scale bars: 1 mm. Lower: representative Masson's Trichrome stained sections of the left ventricles in mice. Scale bars: 100 μm. (K) Quantification of fibrosis area of the heart in mice, $n = 6$ mice per group. (L) Representative immunoblotting images of ETC complex subunits from indicated groups. (M) Representative images of DHE staining of cardiac section in mice. Scale bars: 100 μm, $n = 6$ per group. Data were presented as mean ± SD, *$P < 0.05$, ***$P < 0.001$, ****$P < 0.0001$ vs. HFD + sh-NC group; ##$P < 0.01$, ###$P < 0.001$, ####$P < 0.0001$ vs. HFD + IGK + sh-NC group. Data were analyzed by one-way ANOVA.

and cardiac fibrosis in diet-induced obese mice. A recent study has demonstrated that IGK protected against brain ischemia-reperfusion injury via inhibiting autophagy induced by ER stress [21]. These findings suggested that IGK process versatile health-promoting benefits. As such, our data delivered the first direct evidence of a myocardial protective effects of IGK in obesity-induced metabolic cardiomyopathy. Furthermore, our result revealed that IGK treatment did not elicit obvious signs of toxicity in the liver, kidney or spleen, all of which showed no tissue damage or disturbances on histological analyses. The safety of higher dose of IGK in mice was not addressed in the current

study. Further clinical investigation of the therapeutic potential of IGK in obesity-induced cardiomyopathy are warranted.

Our data verify the hypothesis that the protective effects of IGK are attributable to alleviation of oxidative stress and mitochondrial dysfunction both *in vivo* and *in vitro*. Additionally, IGK treatment significantly decreased LD accumulation and promoted mitochondrial health as revealed by enhanced mitochondrial respiratory capacity and resisting the collapse of mitochondrial membrane potential and oxidative stress. Of note, RNA-sequencing profiling demonstrated that the Nrf2/ARE signaling and mitochondrial respiratory ETC capacity are enriched in the IGK-treated mice. A couple of studies have shown that Nrf2 accelerates mitochondrial fatty acid oxidation and promote mitochondrial health [31,32,43]. In our study, we found that IGK stimulated Nrf2 signaling pathway and resisted mitochondrial dysfunction. Of note, Nrf2 silencing blunted the protection of IGK on cardiac performance and mitochondrial dysfunction both *in vivo* and *in vitro,* indicating that Nrf2 plays a unique role in the IGK mediated protection against obesity MC. Moreover, the findings that IGK did not affect either the random or fasting blood glucose suggested that IGK supplementation attenuated obesity-induced cardiomyopathy independent of regulatory effects on blood glucose.

Nrf2 is a critical regulator of cellular anti-oxidant and anti-inflammatory response, with accumulating evidence describing its role and potential to treat cardiac diseases [44,45]. We add to this argument by showing that IGK as a novel activator of Nrf2/ARE signaling pathway, which significantly attenuated cardiac dysfunction and adverse remodeling in the obese mice. Consistent with our study, pharmacological Nrf2 activation by sulforaphane (SFN) prevented diabetes mellitus-induced cardiac dysfunction [46]. Also, it was reported that empagliflozin ameliorates obesity-related cardiac dysfunction via maintaining redox homeostasis by enhancing Nrf2/HO-1 [47], supported the notion that regulation of Nrf2-mediated genes is influential for the protection against obesity-induced cardiomyopathy.

Nrf2 is considered as an essential antioxidant defense regulator against diverse pathological injuries in the heart; however, there are also evidence showing a detrimental role of Nrf2 in cardiac disease. For example, pressure overload-induced cardiac dysfunction is accelerated in Nrf2-KO mice within first 2 weeks, when myocardial autophagy is intact. However, Nrf2 deficiency ameliorates cardiac hypertrophy and dysfunction throughout the late phase of pressure overload, when the myocardial autophagy is impaired [29]. This finding provides compelling evidence supporting that autophagy impairment turn on Nrf2-driven angiotensinogen (Agt) expression and cardiac maladaptive pathophysiological consequence, which is further supported by a subsequential study using cardiac specific Atg5 and Nrf2 knockout approach [48]. Another recent study from the same group demonstrated a similar phenomenon in type 1 diabetes by showing that autophagy impairment turns off Nrf2-mediated defense while switch on an Nrf2-driven pathological program including Agt activation [30]. In agreement with both studies, an independent group showed that Nrf2-KO mice are characterized by cardiac hypertrophy and diastolic dysfunction but their vascular function is fully protected due to compensatory eNOS elevation [49]. Another study showed that despite of the reduced antioxidant capacity due to Nrf2 deletion, the Nrf2-KO mice were more resistant to myocardial ischemia-reperfusion injury [50]. The author speculated that this was related to the compensatory elevation of eNOS in Nrf2-KO mice, and the protective effect mediated by eNOS was only shown after the Nrf2 signal was blocked [50]. Nrf2-mediated dichotomy in the heart may be attributable to its activation of defense or pathological downstream signaling, or other compensatory mechanism. We found that Agt and Klf9 was increased in the heart of HFD fed mice, however, IGK treatment has minimal effect on Nrf2-operated pathological response in the obese heart (Supplementary material online, Fig. S4). The mechanisms whereby IGK activates Nrf2-mediated antioxidant defense without turning off Nrf2-operated pathological program in the heart warrants further study. Hence,

future studies are warranted to interpret the spatiotemporal role of Nrf2 as well as its target molecular mechanisms in maintaining cardiac homeostasis, which will provide new mechanistic insights into the role of Nrf2 in MC and enlighten the identification of novel therapeutic approaches targeting Nrf2.

Our data revealed that IGK treatment did not alter Nrf2 mRNA level, however it increased Nrf2 protein level and its protein stability. Nrf2 degradation is mainly dependent on the ubiquitin-proteasome system [35]. In support of this notion, we found that IGK promotes the Nrf2 stabilization probably via inhibiting proteasome dependent degradation in light of the recent demonstration of IGK as a general inhibitor of various types of proteasome activity [51]. Keap1, as a physiological inhibitor of Nrf2, is well believed as a negative regulator of Nrf2 protein stability via the cullin3 ubiquitination pathway [52]. However, we did not detect a decrease of Keap1 after IGK treatment. A couple of Keap1-independent Nrf2 degradation mechanisms have been described [53–55]. In support of this, molecular docking analysis showed that IGK entered the pocket of Keap1/Nrf2 complex by 6 H-bond bindings, of which ARG-415 (1.7 Å) shows the higher hydrogen bond binding than the others, implicating that IGK was capable of forming stable conformation with Nrf2. Consistent with our finding, a recent study reported that natural flavonoid quercetin binds to Nrf2 with H-bond of amino acid residues Arg-415, increased the expression of Nrf2 [56]. In addition, a recent study based on molecular docking analysis has revealed a H-bond binding between IGK and HO-1, which is the downstream target of Nrf2 [57], also supporting the antioxidant capacity of IGK.

A few limitations should be considered when interpreting the data reported herein. First, although we demonstrated that IGK treatment conferred protection against obesity-induced MC via Nrf2/ARE antioxidant machinery without affecting blood glucose; however, we cannot totally exclude other possible mechanisms that could contribute to its protection. Second, we revealed the protection of IGK against obesity-induced cardiomyopathy triggered by HFD feeding. However, the benefits of IGK treatment on other types of diabetic cardiomyopathy remain to be elucidated. Last but not least, further studies are warranted to extrapolate our preclinical findings to obese patients with cardiac dysfunction by addressing the therapeutic potential of IGK and IGK-containing herbal preparations.

In conclusion, the present study identifies IGK as a novel naturally-occurring Nrf2 activator from eminent medicinal herb *Ginkgo Biloba*, and demonstrates its safety and efficacy to ameliorate obesity-induced cardiomyopathy.

Author contributions

X.W. and X.Y. conceived the research. X. W and S.X. designed the experiments. X.W., J.H., Y·S., G.Z., C.Y. and Z.L. conduct experiments, acquired and interpretated the data. J.T. and W.Y. performed experiment of Molecular docking and Molecular dynamics simulation. X.W. and J.H. drafted the manuscript. X.Y. and S.X. made critical revision of the manuscript for key intellectual content. All authors discussed the results, commented on the manuscript and final approved the manuscript, and agreed to be accountable for all aspects of the work.

Declaration of competing interest

None.

Data availability

Data will be made available on request.

Acknowledgments

Appendix A. Supplementary data

Supplementary data to this article can be found online at https://doi.org/10.1016/j.redox.2022.102485.

References

[1] C.L. Ogden, C.D. Fryar, C.B. Martin, D.S. Freedman, M.D. Carroll, Q. Gu, C. M. Hales, Trends in obesity prevalence by race and hispanic origin-1999-2000 to 2017-2018, JAMA 324 (12) (2020) 1208–1210.

[2] C. Maack, E. Murphy, Metabolic cardiomyopathies - fighting the next epidemic, Cardiovasc. Res. 113 (4) (2017) 367–369.

[3] E.D. Abel, S.E. Litwin, G. Sweeney, Cardiac remodeling in obesity, Physiol. Rev. 88 (2) (2008) 389–419.

[4] J. Ren, N.N. Wu, S. Wang, J.R. Sowers, Y. Zhang, Obesity cardiomyopathy: evidence, mechanisms, and therapeutic implications, Physiol. Rev. 101 (4) (2021) 1745–1807.

[5] A. Aminian, R. Wilson, A. Zajichek, C. Tu, K.E. Wolski, P.R. Schauer, M.W. Kattan, S.E. Nissen, S.A. Brethauer, Cardiovascular outcomes in patients with type 2 diabetes and obesity: comparison of gastric bypass, sleeve gastrectomy, and usual Care, Diabetes Care 44 (11) (2021) 2552–2563.

[6] T.A. McDonagh, M. Metra, M. Adamo, R.S. Gardner, A. Baumbach, M. Böhm, H. Burri, J. Butler, J. Čelutkienė, O. Chioncel, J.G.F. Cleland, A.J.S. Coats, M. G. Crespo-Leiro, D. Farmakis, M. Gilard, S. Heymans, A.W. Hoes, T. Jaarsma, E. A. Jankowska, M. Lainscak, C.S.P. Lam, A.R. Lyon, J.J.V. McMurray, A. Mebazaa, R. Mindham, C. Muneretto, M. Francesco Piepoli, S. Price, G.M.C. Rosano, F. Ruschitzka, A. Kathrine Skibelund, ESC Guidelines for the diagnosis and treatment of acute and chronic heart failure, Eur. Heart J. 42 (36) (2021) 3599–3726, 2021.

[7] M. Obokata, Y.N.V. Reddy, S.V. Pislaru, V. Melenovsky, B.A. Borlaug, Evidence supporting the existence of a distinct obese phenotype of heart failure with preserved ejection fraction, Circulation 136 (1) (2017) 6–19.

[8] J. Ren, M. Sun, H. Zhou, A. Ajoolabady, Y. Zhou, J. Tao, J.R. Sowers, Y. Zhang, FUNDC1 interacts with FBXL2 to govern mitochondrial integrity and cardiac function through an IP3R3-dependent manner in obesity, Sci. Adv. 6 (38) (2020).

[9] S. Boudina, S. Sena, B.T. O'Neill, P. Tathireddy, M.E. Young, E.D. Abel, Reduced mitochondrial oxidative capacity and increased mitochondrial uncoupling impair myocardial energetics in obesity, Circulation 112 (17) (2005) 2686–2695.

[10] S. Boudina, S. Sena, H. Theobald, X. Sheng, J.J. Wright, X.X. Hu, S. Aziz, J. I. Johnson, H. Bugger, V.G. Zaha, E.D. Abel, Mitochondrial energetics in the heart in obesity-related diabetes: direct evidence for increased uncoupled respiration and activation of uncoupling proteins, Diabetes 56 (10) (2007) 2457–2466.

[11] J.J. Rayner, M.A. Peterzan, W.D. Watson, W.T. Clarke, S. Neubauer, C.T. Rodgers, O.J. Rider, Myocardial energetics in obesity: enhanced ATP delivery through creatine kinase with blunted stress response, Circulation 141 (14) (2020) 1152–1163.

[12] M. Chattopadhyay, I. Guhathakurta, P. Behera, K.R. Ranjan, M. Khanna, S. Mukhopadhyay, S. Chakrabarti, Mitochondrial bioenergetics is not impaired in nonobese subjects with type 2 diabetes mellitus, Metab. Clin. Exp. 60 (12) (2011) 1702–1710.

[13] P.M. Miotto, P.J. LeBlanc, G.P. Holloway, High-fat diet causes mitochondrial dysfunction as a result of impaired ADP sensitivity, Diabetes 67 (11) (2018) 2199–2205.

[14] Q. Ma, Role of nrf2 in oxidative stress and toxicity, Annu. Rev. Pharmacol. Toxicol. 53 (2013) 401–426.

[15] K. Kleszczyński, D. Zillikens, T.W. Fischer, Melatonin enhances mitochondrial ATP synthesis, reduces reactive oxygen species formation, and mediates translocation of the nuclear erythroid 2-related factor 2 resulting in activation of phase-2 antioxidant enzymes (γ-GCS, HO-1, NQO1) in ultraviolet radiation-treated normal human epidermal keratinocytes (NHEK), J. Pineal Res. 61 (2) (2016) 187–197.

[16] Y. Fang, J. Ye, B. Zhao, J. Sun, N. Gu, X. Chen, L. Ren, J. Chen, X. Cai, W. Zhang, Y. Yang, P. Cao, Formononetin ameliorates oxaliplatin-induced peripheral neuropathy via the KEAP1-NRF2-GSTP1 axis, Redox Biol. 36 (2020), 101677.

[17] Z. Yu, W. Shao, Y. Chiang, W. Foltz, Z. Zhang, W. Ling, I.G. Fantus, T. Jin, Oltipraz upregulates the nuclear factor (erythroid-derived 2)-like 2 [corrected](NRF2) antioxidant system and prevents insulin resistance and obesity induced by a high-fat diet in C57BL/6J mice, Diabetologia 54 (4) (2011) 922–934.

[18] B. Korac, A. Kalezic, V. Pekovic-Vaughan, A. Korac, A. Jankovic, Redox changes in obesity, metabolic syndrome, and diabetes, Redox Biol. 42 (2021), 101887.

[19] F. Briançon-Scheid, A. Lobstein-Guth, R. Anton, HPLC separation and quantitative determination of biflavones in leaves from Ginkgo biloba, Planta Med. 49 (12) (1983) 204–207.

[20] X. Li, X. Ouyang, R. Cai, D. Chen, 3′,8″-Dimerization enhances the antioxidant capacity of flavonoids: evidence from acacetin and isoginkgetin, Molecules 24 (11) (2019).

[21] Y. Li, L. Meng, B. Li, D. Huang, X. Huang, C. Lin, D. Li, S. Qiu, Y. Wu, Z. Wei, X. Li, Isoginkgetin attenuates endoplasmic reticulum stress-induced autophagy of brain after ischemic reperfusion injury, Bioengineered (2021), https://doi.org/10.1080/21655979.2021.1997564. Epub ahead of print. PMID: 34787074.

[22] M. Tong, T. Saito, P. Zhai, S.I. Oka, W. Mizushima, M. Nakamura, S. Ikeda, A. Shirakabe, J. Sadoshima, Mitophagy is essential for maintaining cardiac function during high fat diet-induced diabetic cardiomyopathy, Circ. Res. 124 (9) (2019) 1360–1371.

[23] D. Zheng, Z. Liu, Y. Zhou, N. Hou, W. Yan, Y. Qin, Q. Ye, X. Cheng, Q. Xiao, Y. Bao, J. Luo, X. Wu, B. Urolithin, A gut microbiota metabolite, protects against myocardial ischemia/reperfusion injury via p62/Keap1/Nrf2 signaling pathway, Pharmacol. Res. 153 (2020), 104655.

[24] M. Nakamura, T. Liu, S. Husain, P. Zhai, J.S. Warren, C.P. Hsu, T. Matsuda, C. J. Phiel, J.E. Cox, B. Tian, H. Li, J. Sadoshima, Glycogen synthase kinase-3α promotes fatty acid uptake and lipotoxic cardiomyopathy, Cell Metabol. 29 (5) (2019) 1119–1134, e12.

[25] S. Sciarretta, P. Zhai, D. Shao, Y. Maejima, J. Robbins, M. Volpe, G. Condorelli, J. Sadoshima, Rheb is a critical regulator of autophagy during myocardial ischemia: pathophysiological implications in obesity and metabolic syndrome, Circulation 125 (9) (2012) 1134–1146.

[26] D. Shao, S.C. Kolwicz Jr., P. Wang, N.D. Roe, O. Villet, K. Nishi, Y.A. Hsu, G. V. Flint, A. Caudal, W. Wang, M. Regnier, R. Tian, Increasing fatty acid oxidation prevents high-fat diet-induced cardiomyopathy through regulating parkin-mediated mitophagy, Circulation 142 (10) (2020) 983–997.

[27] Z. Li, Z. Guo, R. Lan, S. Cai, Z. Lin, J. Li, J. Wang, Z. Li, P. Liu, The poly(ADP-ribosyl)ation of BRD4 mediated by PARP1 promoted pathological cardiac hypertrophy, Acta Pharm. Sin. B 11 (5) (2021) 1286–1299.

[28] M. Brownlee, Biochemistry and molecular cell biology of diabetic complications, Nature 414 (6865) (2001) 813–820.

[29] Q. Qin, C. Qu, T. Niu, H. Zang, L. Qi, L. Lyu, X. Wang, M. Nagarkatti, P. Nagarkatti, J.S. Janicki, X.L. Wang, T. Cui, Nrf2-Mediated cardiac maladaptive remodeling and dysfunction in a setting of autophagy insufficiency, Hypertension 67 (1) (2016) 107–117.

[30] H. Zang, W. Wu, L. Qi, W. Tan, P. Nagarkatti, M. Nagarkatti, X. Wang, T. Cui, Autophagy inhibition enables Nrf2 to exaggerate the progression of diabetic cardiomyopathy in mice, Diabetes 69 (12) (2020) 2720–2734.

[31] M.H. Ludtmann, P.R. Angelova, Y. Zhang, A.Y. Abramov, A.T. Dinkova-Kostova, Nrf2 affects the efficiency of mitochondrial fatty acid oxidation, Biochem. J. 457 (3) (2014) 415–424.

[32] J.D. Hayes, A.T. Dinkova-Kostova, The Nrf2 regulatory network provides an interface between redox and intermediary metabolism, Trends Biochem. Sci. 39 (4) (2014) 199–218.

[33] F.A. Neves, E. Cortez, A.F. Bernardo, A.B. Mattos, A.K. Vieira, O. Malafaia Tde, A. A. Thole, A.C. Rodrigues-Cunha, E.P. Garcia-Souza, R. Sichieri, A.S. Moura, Heart energy metabolism impairment in Western-diet induced obese mice, J. Nutr. Biochem. 25 (1) (2014) 50–57.

[34] I. Dikic, Proteasomal and autophagic degradation systems, Annu. Rev. Biochem. 86 (2017) 193–224.

[35] M. Yamamoto, T.W. Kensler, H. Motohashi, The KEAP1-NRF2 system: a thiol-based sensor-effector apparatus for maintaining redox homeostasis, Physiol. Rev. 98 (3) (2018) 1169–1203.

[36] A.C.T. Ng, V. Delgado, B.A. Borlaug, J.J. Bax, Diabesity: the combined burden of obesity and diabetes on heart disease and the role of imaging, Nat. Rev. Cardiol. 18 (4) (2021) 291–304.

[37] M.A. Alpert, C.J. Lavie, H. Agrawal, K.B. Aggarwal, S.A. Kumar, Obesity and heart failure: epidemiology, pathophysiology, clinical manifestations, and management, Transl. Res. : J. Lab. Clin. Med. 164 (4) (2014) 345–356.

[38] A.H. Nguyen, J.U. Lee, S.J. Sim, Nanoplasmonic probes of RNA folding and assembly during pre-mRNA splicing, Nanoscale 8 (8) (2016) 4599–4607.

[39] X.J. Zhang, Y.X. Ji, X. Cheng, Y. Cheng, H. Yang, J. Wang, L.P. Zhao, Y.P. Huang, D. Sun, H. Xiang, L.J. Shen, P.L. Li, J.P. Ma, R.F. Tian, J. Yang, X. Yao, H. Xu, R. Liao, L. Xiao, P. Zhang, X. Zhang, G.N. Zhao, X. Wang, M.L. Hu, S. Tian, J. Wan, J. Cai, X. Ma, Q. Xu, Y. Wang, R.M. Touyz, P.P. Liu, R. Loomba, Z.G. She, H. Li, A small molecule targeting ALOX12-ACC1 ameliorates nonalcoholic steatohepatitis in mice and macaques, Sci. Transl. Med. 13 (624) (2021), eabg8116.

[40] M. Li, B. Li, Y. Hou, Y. Tian, L. Chen, S. Liu, N. Zhang, J. Dong, Anti-inflammatory effects of chemical components from Ginkgo biloba L. male flowers on lipopolysaccharide-stimulated RAW264.7 macrophages, Phytother Res. 33 (4) (2019) 989–997.

[41] R. Darrigrand, A. Pierson, M. Rouillon, D. Renko, D. Boulpicante, D. Bouyssié, E. Mouton-Barbosa, J. Marcoux, C. Garcia, M. Ghosh, M. Alami, S. Apcher, Isoginkgetin derivative IP2 enhances the adaptive immune response against tumor antigens, Commun Biol 4 (1) (2021) 269.

[42] M. Li, B. Li, Z.M. Xia, Y. Tian, D. Zhang, W.J. Rui, J.X. Dong, F.J. Xiao, Anticancer effects of five biflavonoids from Ginkgo biloba L. Male flowers in vitro, Molecules 24 (8) (2019).

[43] A.T. Dinkova-Kostova, A.Y. Abramov, The emerging role of Nrf2 in mitochondrial function, Free Radic. Biol. Med. 88 (2015) 179–188.

[44] B.K. Ooi, K.G. Chan, B.H. Goh, W.H. Yap, The role of natural products in targeting cardiovascular diseases via Nrf2 pathway: novel molecular mechanisms and therapeutic approaches, Front. Pharmacol. 9 (2018) 1308.

[45] H. Ashrafian, G. Czibik, M. Bellahcene, D. Aksentijević, A.C. Smith, S.J. Mitchell, M.S. Dodd, J. Kirwan, J.J. Byrne, C. Ludwig, H. Isackson, A. Yavari, N.B. Støttrup, H. Contractor, T.J. Cahill, N. Sahgal, D.R. Ball, R.I. Birkler, I. Hargreaves, D. A. Tennant, J. Land, C.A. Lygate, M. Johanssen, R.K. Kharbanda, S. Neubauer, C. Redwood, R. de Cabo, I. Ahmet, M. Talan, U.L. Günther, A.J. Robinson, M. R. Viant, P.J. Pollard, D.J. Tyler, H. Watkins, Fumarate is cardioprotective via activation of the Nrf2 antioxidant pathway, Cell Metabol. 15 (3) (2012) 361–371.

[46] J. Gu, Y. Cheng, H. Wu, L. Kong, S. Wang, Z. Xu, Z. Zhang, Y. Tan, B.B. Keller, H. Zhou, Y. Wang, Z. Xu, L. Cai, Metallothionein is downstream of Nrf2 and

partially mediates sulforaphane prevention of diabetic cardiomyopathy, Diabetes 66 (2) (2017) 529–542.

[47] X. Sun, F. Han, Q. Lu, X. Li, D. Ren, J. Zhang, Y. Han, Y.K. Xiang, J. Li, Empagliflozin ameliorates obesity-related cardiac dysfunction by regulating sestrin2-mediated AMPK-mTOR signaling and redox homeostasis in high-fat diet-induced obese mice, Diabetes 69 (6) (2020) 1292–1305.

[48] W. Wu, Q. Qin, Y. Ding, H. Zang, D.S. Li, M. Nagarkatti, P. Nagarkatti, W. Wang, X. Wang, T. Cui, Autophagy controls nrf2-mediated dichotomy in pressure overloaded hearts, Front. Physiol. 12 (2021), 673145.

[49] R. Erkens, C.M. Kramer, W. Lückstädt, C. Panknin, L. Krause, M. Weidenbach, J. Dirzka, T. Krenz, E. Mergia, T. Suvorava, M. Kelm, M.M. Cortese-Krott, Left ventricular diastolic dysfunction in Nrf2 knock out mice is associated with cardiac hypertrophy, decreased expression of SERCA2a, and preserved endothelial function, Free Radic. Biol. Med. 89 (2015) 906–917.

[50] R. Erkens, T. Suvorava, T.R. Sutton, B.O. Fernandez, M. Mikus-Lelinska, F. Barbarino, U. Flögel, M. Kelm, M. Feelisch, M.M. Cortese-Krott, Nrf2 Deficiency Unmasks the Significance of Nitric Oxide Synthase Activity for Cardioprotection, Oxidative Medicine and Cellular Longevity 2018, 2018, 8309698.

[51] J. Tsalikis, M. Abdel-Nour, A. Farahvash, M.T. Sorbara, S. Poon, D.J. Philpott, S. E. Girardin, Isoginkgetin, a natural biflavonoid proteasome inhibitor, sensitizes cancer cells to apoptosis via disruption of lysosomal homeostasis and impaired protein clearance, Mol. Cell Biol. 39 (10) (2019).

[52] C. Meng, J. Zhan, D. Chen, G. Shao, H. Zhang, W. Gu, J. Luo, The deubiquitinase USP11 regulates cell proliferation and ferroptotic cell death via stabilization of NRF2 USP11 deubiquitinates and stabilizes NRF2, Oncogene 40 (9) (2021) 1706–1720.

[53] Y. Wang, R. Jin, J. Chen, J. Cao, J. Xiao, X. Li, C. Sun, Tangeretin maintains antioxidant activity by reducing CUL3 mediated NRF2 ubiquitination, Food Chem. 365 (2021), 130470.

[54] H. Zhou, J. Lu, K. Chinnaswamy, J.A. Stuckey, L. Liu, D. McEachern, C.Y. Yang, D. Bernard, H. Shen, L. Rui, Y. Sun, S. Wang, Selective inhibition of cullin 3 neddylation through covalent targeting DCN1 protects mice from acetaminophen-induced liver toxicity, Nat. Commun. 12 (1) (2021) 2621.

[55] S. Huang, T. He, S. Yang, H. Sheng, X. Tang, F. Bao, Y. Wang, X. Lin, W. Yu, F. Cheng, W. Lv, J. Hu, Metformin reverses chemoresistance in non-small cell lung cancer via accelerating ubiquitination-mediated degradation of Nrf2, Transl. Lung Cancer Res. 9 (6) (2020) 2337–2355.

[56] L.L. Ji, Y.C. Sheng, Z.Y. Zheng, L. Shi, Z.T. Wang, The involvement of p62-Keap1-Nrf2 antioxidative signaling pathway and JNK in the protection of natural flavonoid quercetin against hepatotoxicity, Free Radic. Biol. Med. 85 (2015) 12–23.

[57] P. Santhakumar, L. Prathap, A. Roy, S. Jayaraman, M. Jeevitha, Molecular docking analysis of furfural and isoginkgetin with heme oxygenase I and PPARγ, Bioinformation 17 (2) (2021) 356–362.